Heat of Formation of the Allyl Ion by TPEPICO Spectroscopy

Nicholas S. Shuman,[†] William R. Stevens, Katherine Lower, and Tomas Baer*

Department of Chemistry, The University of North Carolina at Chapel Hill, Chapel Hill, North Carolina 27599

Received: July 15, 2009; Revised Manuscript Received: August 16, 2009

The 0 K onset of $C_3H_6 \rightarrow C_3H_5^+ + H^\bullet$ is measured by threshold photoelectron−photoion coincidence (TPEPICO) spectroscopy. From the onset (11.898 ± 0.025 eV) the heat of formation of the allyl ion ($CH_2CHCH_2^+$) is determined to be $\Delta H°_{f,0K} = 967.2$; $\Delta H°_{f,298K} = 955.4 \pm 2.5$ kJ mol^{-1}. The value is significantly more positive than prior determinations, and resolves a discrepancy between measurements of the allyl radical and allyl ion heats of formation and recent highly precise measurements of the allyl radical adiabatic ionization energy. The new allyl ion heat of formation leads to a new proton affinity for propadiene (allene) of 765.0 ± 2.6 kJ mol^{-1}. An attempt is made to determine the $CH_3CCH_2^+$ heat of formation by measuring the 0 K onset of 2-$ClC_3H_5 \rightarrow C_3H_5^+ + Cl^\bullet$. However, $C_3H_5^+$ appears at too low an energy to be the higher energy $CH_3CCH_2^+$ structure. Rather, 2-$ClC_3H_5^+$ undergoes a concerted hydrogen transfer and Cl-loss via an intramolecular S_N2 like mechanism to produce the allyl ion. The 0 K onset of 3-$ClC_3H_5 \rightarrow C_3H_5^+ + Cl^\bullet$ (11.108 ± 0.010 eV) is measured to determine the 3-ClC_3H_5 heat of formation ($\Delta H°_{f,0K} = 14.9$; $\Delta H°_{f,298K} = 1.1 \pm 2.7$ kJ mol^{-1}). 3-$ClC_3H_5^+$ is suggested to readily isomerize to trans 1-$ClC_3H_5^+$ prior to dissociation.

Introduction

The allyl radical ($CH_2CHCH_2^\bullet$) and allyl ion ($CH_2CHCH_2^+$) are the lowest energy isomers of $C_3H_5^\bullet$ and $C_3H_5^+$. Both species are key intermediates in combustion and interstellar chemistry, and as a result their energetics have been the subject of numerous experimental and theoretical studies.[1−16] Recently, the adiabatic ionization energy of $CH_2CHCH_2^\bullet$, which defines the energy difference between the ground states of the radical and the ion, has been measured by pulsed field ionization photoelectron (PFI-PE) spectroscopy.[10,17] Because of the tremendous precision of the reported values (8.13146 ± 0.00025 eV,[10] 8.13090 ± 0.00025 eV[17]), an accurate determination of the heat of formation of either the allyl radical or ion effectively determines the heats of formation of both.

Inspection of the many measurements of the heats of formation of allyl radical and ion reveals a discrepancy with the PFI-PE ionization energy. Reported 298 K heats of formation of the radical include 163.6 ± 6,[2] 164.8 ± 6,[3] 167.4 ± 4,[18] 171 ± 4,[4] and 173.2 ± 2.1[1] kJ mol^{-1}. The two most positive values, a shock tube measurement by Tsang and Walker[4] and a series of equilibrium measurements using a selected ion flow tube by Ellison et al.,[1] are the most recent determinations and appear to be more reliable than the older measurements with which they disagree. These two values suggest a 298 K heat of formation of 173 ± 2 kJ mol^{-1}.

Measured 298 K heats of formation of the ion, each determined from the appearance energies of $C_3H_5^+$ from various precursors, include 939.3 ± 4,[7] 946 ± 8.5,[6] 949.6 ± 1.4,[5] and 971 ± 12[8] kJ mol^{-1}. All of these values are derived from photoionization mass spectrometry (PIMS) or energy selected electron impact measurements of the appearance energy of $C_3H_5^+$ from various precursors. The most recent (although dating to 1984), and by far the most precisely reported value, is that of Traeger,[5] derived from PIMS measurements on six alkane and alkene species. Additionally, Holmes et al. review a series of electron impact measurements and suggests a 298 K heat of formation of 941 ± 10 kJ mol^{-1}.[19]

These 298 K heats of formation may be converted to the 0 K values using the standard thermochemical cycle, and the difference between the ion and radical heats of formation compared to the well-determined adiabatic ionization energy. The literature 0 K heats of formation of allyl radical ($\Delta H°_{f,298K} = 184.6 \pm 2.0$ kJ mol^{-1}) and ion ($\Delta H°_{f,0K} = 961.4 \pm 1.4$ kJ mol^{-1}), using the measurements of Tsang[4] and Ellison[1] for the radical and Traeger[5] for the ion, differ by 8.052 ± 0.025 eV. This is 80 meV (8 kJ mol^{-1}) less than the known IE, a discrepancy that is well outside of the reported uncertainties of the measurements. These literature heats of formation of the allyl radical and ion cannot both be correct.

Inspection of all the reported values quickly reveals that the Traeger number is on the upper end of reported allyl ion heats of formation, and is in quite good agreement with the older allyl radical heats of formation, which are between 5 and 10 kJ mol^{-1} more negative than the Ellison/Tsang value, whereas the Ellison/Tsang value is in poor agreement with all reported allyl ion heats of formation. While this would suggest that it is the radical heat of formation that is in error, we believe that it is more likely that the reported allyl ion heats of formation are significantly more negative than the true value.

Determination of an ion heat of formation by PIMS requires measuring the 0 K thermochemical threshold (E_0) of

$$RC_3H_5 \rightarrow R^\bullet + C_3H_5^+ \qquad (1)$$

and knowledge of the heats of formation of the corresponding neutral and radical species. In practice this involves monitoring the mass signal corresponding to the ion while continuously scanning the photon energy in order to produce a photoionization curve. The appearance energy (AE) of the ion is determined by extrapolating a linear portion of the photoionization curve down to the baseline.[20] There may be ambiguity as to what region of the curve should be deemed linear, and the assignment can have

[†] Current address: Air Force Research Laboratory, Space Vehicles Directorate, 29 Randolph Road, Hanscom Air Force Base, MA 01731-3010.

10.1021/jp906691a CCC: $40.75 © 2009 American Chemical Society
Published on Web 09/11/2009

a large effect on the derived AE. Additionally, the AE is a function of the thermal energy distribution of the ion and depends on the temperature of the sample, so that some assumptions are required to extract the 0 K E_0. Although the thermal energy of the neutral can be accurately determined from the sample temperature, the resulting ion internal energy distribution depends on Franck−Condon factors. Thus the conversion of the room temperature AE to the E_0 is not straightforward and, as temperature dependent PIMS studies of a large number of molecules have shown, large errors can arise for certain molecules.[20] Finally, the PIMS method does not contain sufficient information to make corrections for possible kinetic or competitive shifts[21] for the $C_3H_5^+$ appearance energies.

Much more precise measurements of E_0 may be made by energy selecting the dissociating ions, as is done in threshold photoelectron−photoion coincidence (TPEPICO) spectroscopy. Of the numerous species which dissociate to produce $C_3H_5^+$, most have either poorly determined heats of formation themselves (e.g., C_3H_5X (X = Cl, Br, I), c-C_3H_6) or have a competing lower energy dissociation channel, which complicates the analysis. Examples of the latter are various isomers of C_4H_8. The most appropriate precursor is propene, which has a very well-defined heat of formation ($\Delta H°_{f,298K}$ = 20.0 ± 0.7 kJ mol^{-1})[22] and for which H-loss is the lowest energy dissociation channel. The H-loss pathway for propene ion dissociation is certainly to the lowest energy $C_3H_5^+$ isomer, namely the allyl ion,[19] and here we measure the E_0 of this process by TPEPICO spectroscopy in order to accurately determine the allyl ion heat of formation.

There is evidence that suggests that the lowest energy isomers of $C_3H_5^+$, the more stable allyl ion ($CH_2CHCH_2^+$) and the 2-propenyl ion ($CH_3CCH_2^+$), have a sufficiently high barrier to interconversion that isomerization will not readily occur.[23] It could thus be hoped that Cl-loss from 2-chloropropene and 3-chloropropene would produce the two different stable isomers. The only literature values of the 3-chloropropene heat of formation we are aware of are one derived from a PIMS measurement,[5] the precision of which would be significantly improved by determination of E_0 by TPEPICO, and an older value listed in the compilation of Stull et al.[24] derived from an early combustion calorimetry measurement[25] and an electron impact study.[26] The 2-chloropropene heat of formation has been determined by equilibrium measurements.[22,27] If this ion were to dissociate via a simple C−Cl bond cleavage, its dissociation energy, E_0, could be used to determine the 2-propenyl ion heat of formation. Here we will show that, unfortunately, this is not the case. Although the $C_3H_5^+$ product isomers likely do not isomerize, the $ClC_3H_5^+$ isomers do, and the 2-chloropropene ion does not dissociate to the 2-propenyl ion, but rather to the allyl ion, precluding an experimental determination of its heat of formation by this method.

Experimental and Computational Methods

The TPEPICO experiment has been described in detail elsewhere.[28−30] Sample vapor is equilibrated at a variable temperature between 215 and 400 K in transit through approximately 12 in. of copper tubing and enters a high vacuum chamber through a stainless steel needle. Vacuum ultraviolet (VUV) radiation from a hydrogen discharge lamp source dispersed by a 1 m normal incidence monochromator (resolution 8 meV at 10 eV) intersects the effusive beam. Photon energies are selected to ionize or dissociatively ionize the neutral species. Ions and electrons are accelerated in opposite directions by a uniform voltage field of 22 V cm^{-1}. Electrons are velocity focused such that those with zero kinetic energy transverse to the acceleration axis (including both zero kinetic energy electrons and those with an initial velocity directed entirely along the acceleration axis) are detected by a Channeltron electron multiplier located on-axis and masked by a 1.4 mm aperture. A representative portion of energetic electrons are detected by another Channeltron located off-axis and masked by a 2 × 6 mm rectangular aperture. The off-axis signal is used in a scheme to subtract off the excited electron contribution to the on-axis signal.

Ions enter one of two space focused time-of-flight (TOF) mass spectrometer setups. One, a linear TOF (LinTOF) mass spectrometer, consists of an initial 4.8 cm acceleration region that accelerates the ions to 100 eV, followed by a steeper 2 mm acceleration region to 260 eV. The ions then pass through a 26 cm field-free drift region. Prior to detection by a tandem microchannel plate detector, the ions are decelerated in order to separate the flight times of ion fragments produced in the drift region and undissociated parent ions. The second setup, a reflectron TOF (ReTOF) mass spectrometer, consists of the same 4.8 cm acceleration region. The ions then drift at 100 eV for about 37 cm, are reflected by a 22 cm long reflector and drift at 100 eV for another 35 cm.

In both setups, time zero of the TOF is determined by detection of an electron on either the on- or off-axis detector. After subtraction of the energetic electron signal, the TOF spectra consist solely of events that produced zero kinetic energy electrons. As a result, the internal energy of the parent ions is well determined by the sum of the photon energy and the initial thermal energy.

All calculations were performed with the Gaussian 03 quantum chemical software package.[31] Density and number of states were calculated by the Beyer−Sweinhart direct count method using unscaled[32] vibrational frequencies and rotational constants determined from geometries optimized at the B3LYP/6-311++G(d,p) level. Calculated thermochemical values are those determined using either the G3B3[33] or CBS-APNO[34] model chemistries.

Results and Analysis

I. Propene. As shown in the breakdown diagram (the relative abundances of parent and daughter ions as a function of photon energy) in Figure 1, internally excited propene ions dissociate through two competing channels: H-loss to form $C_3H_5^+$, and H_2-loss to form $C_3H_4^+$. We assume that the H-loss occurs through a simple bond cleavage and that the product channel is accessible at its thermochemical threshold. The H_2-loss must occur with a substantial reverse barrier, as the enthalpy of formation of $C_3H_4^+$ [22,35] is well-established, and the threshold to this channel is several eV lower in energy than the appearance of the product ion. As a result, thermochemical data may be extracted from the onset of the H-loss channel only, and the H_2-loss channel is considered only insofar as it is necessary to the modeling that determines the E_0 of the H-loss channel.

Typically, bond cleavages in small ions occur with rate constants much faster than the microsecond time scale of mass spectrometry measurements. However, due to the high strength of the C−H bond in the propene ion, the H-loss occurs with a minimum rate constant of 10^4−10^5 s^{-1} resulting in metastable parent ions. The fraction of propene ions that dissociate is a function of not only the internal energy distribution of the ions but also the time required to extract the ions and detect them. It is thus necessary to obtain dissociation rate information in order to model the breakdown diagram. The dissociation rate

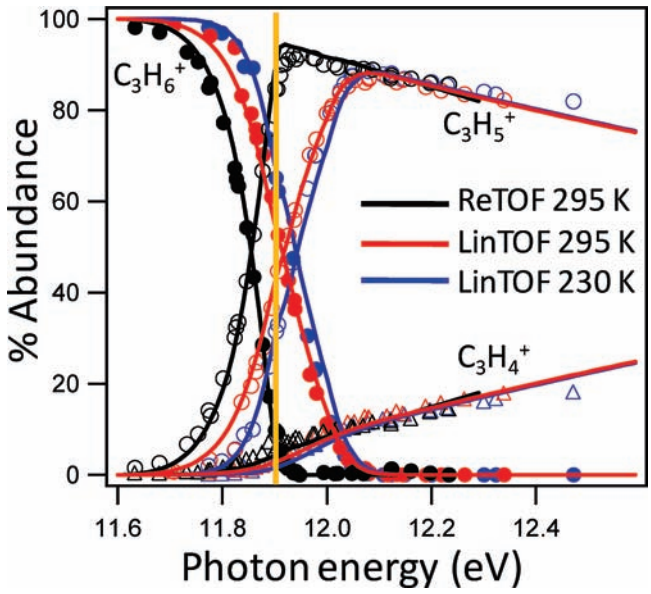

Figure 1. Breakdown diagrams of propene taken under the indicated conditions. Circles and triangles are experimental points, and lines are best-fit simulations using identical parameters (see text). The E_0 of the H-loss channel at 11.898 ± 0.025 eV is indicated by the yellow line.

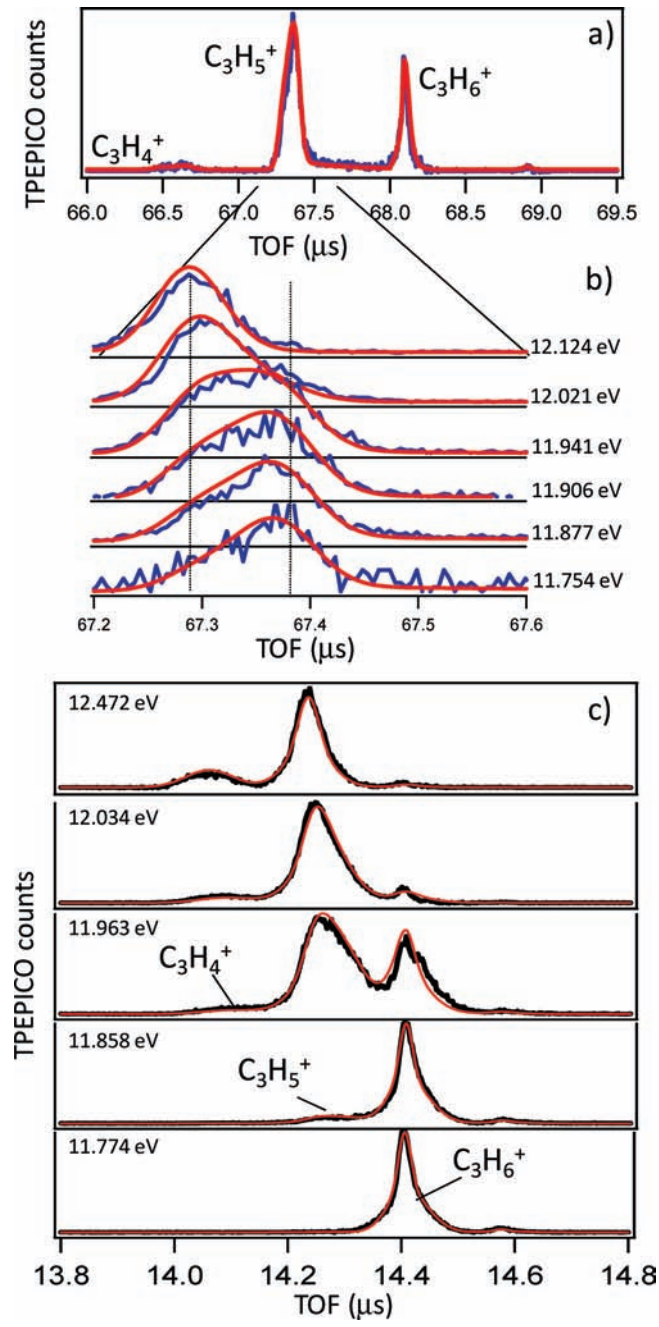

Figure 2. (a) Representative experimental (blue) and simulated (red) ReTOF spectra of propene at 11.877 eV. (b) Expanded section of ReTOF spectra showing the $C_3H_5^+$ daughter peak at the indicated photon energies. The dissociation rate is reflected by the shifting of the center-of-mass of the peak (see text). (c) Representative experimental (black) and simulated (red) LinTOF spectra of propene at 235 K at the indicated photon energies.

can be obtained from the asymmetric daughter ion peaks in the TOF spectra (Figure 2). This asymmetry is due to parent ions dissociating along the entire length of the first acceleration region, and therefore reflects the fraction of dissociated ions as a function of flight time. Because of the 1 amu difference between the parent and daughter ions, the asymmetric daughter ion peak in the LinTOF setup is not fully resolved from the parent ion peak. To ensure the reliability of our modeled fit, data were taken under several conditions: using the LinTOF mass spectrometer with the sample at both room temperature and 230 K (thereby varying the ion internal energy distribution), and using the ReTOF mass spectrometer at room temperature. The peaks in the ReTOF data are fully resolved, however the asymmetry of the daughter peaks is less pronounced (and therefore more difficult to accurately model). The interpretation of the peak shapes in the ReTOF spectra is not obvious. The symmetric peak at 68.1 μs is the parent $C_3H_6^+$ ion, and the small peak at 68.9 μs is its corresponding ^{13}C isotopomer. The peaks at approximately 66.6 and 67.4 μs correspond to the daughter $C_3H_4^+$ and $C_3H_5^+$ peaks respectively, and each consists of two mostly unresolved peaks (more clearly seen for the $C_3H_5^+$ peak in Figure 2b). Ions dissociating to $C_3H_5^+$ immediately upon ionization appear at 67.3 μs, while ions dissociating after already traveling some distance along the acceleration region appear at slightly longer times-of-flight between 67.3 and 67.4 μs. Ions dissociating in the field-free drift region all appear at 67.4 μs with a peak width determined primarily by the kinetic energy release of the dissociation. Much of the rate information in the ReTOF spectra is contained in the relative areas of the "acceleration region" and "drift region" peaks and, because the peaks are not fully resolved, is manifested as a shift in the center-of-mass of the entire peak. At higher photon energies, the dissociation rate is higher and a larger fraction of ions dissociate within the initial acceleration region, as shown by the experimental and best-fit simulated spectra in Figure 2b. Finally, ions which dissociate within the reflectron appear at TOFs between the more apparent daughter and parent ion peaks, and can be seen as an elevated, sloping baseline in Figure 2a.

Rate information is also obtained from the significantly different draw-out times of the two mass spectrometer setups: 4.4 μs for the LinTOF and 22 μs for the ReTOF. Because the minimum rate constant of the H-loss channel happens to be on the order of tens of microseconds, the kinetic shifts in the LinTOF and ReTOF data differ significantly: roughly 150 meV in the LinTOF, but almost zero in the ReTOF.

Unimolecular rate theory is needed to model the relative rates of the two dissociation pathways. Because the H-loss occurs with no energetic barrier, the system does not have a well-defined transition state, so that the Rice−Ramsperger−Kassel−Marcus (RRKM) theory[36] cannot be used to accurately model this reaction rate. Variational transition state theory (VTST)[37,38] or the statistical adiabatic channel model (SACM)[39] are most

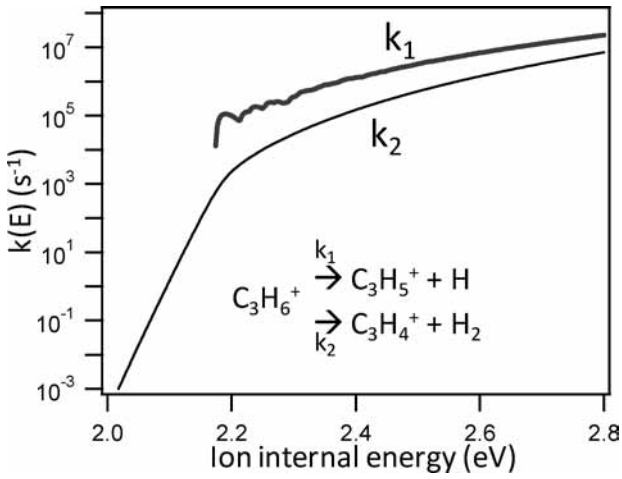

Figure 3. Dissociation rate curves of propene ions via H-loss and H_2 elimination as determined by modeling (see text). The oscillations in the H loss rate curve at low energies are a result of the sparse vibrational state density in the product ion.

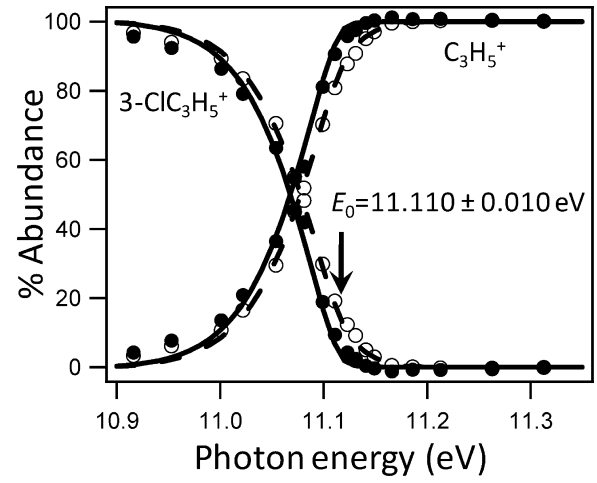

Figure 4. Breakdown diagrams of 3-ClC_3H_5 at 235 K. Experimentally observed abundances and best-fit simulation are shown for ion dissociations occurring within 5.9 μs of ionization (open circles, dashed lines) and those occurring within 16.3 μs (filled circles, solid lines).

appropriate to describe the dissociation, however both methods require arduous calculation. Instead, we employ a simplified version of the statistical adiabatic channel model (SSACM),[40] which has been shown to effectively model a range of unimolecular ionic dissociations,[40,41] in order to model the H-loss rate curve. The H_2-loss does proceed over a barrier and has a well-defined transition state so that we model it using RRKM theory and tunneling through the barrier is modeled by assuming an Eckart potential.[36] The details of modeling parallel dissociation pathways in a TPEPICO experiment in order to determine E_0's have been discussed in detail elsewhere.[42] The best fit simulations to the breakdown diagrams in Figure 1 and the TOF distributions in Figure 2, which take into account the rate constants and the ion thermal energy distribution, are obtained with the specific rate curves shown in Figure 3. This yields an $E_0 = 11.898 \pm 0.025$ eV. The Traeger 298 K PIMS onset of 11.86 ± 0.01 eV can be converted to a 0 K E_0 value of 11.93 eV by adding the propene thermal vibrational and rotational energy of 0.07 eV. Our lower energy is clearly a result of the kinetic shift that was not taken into account by Traeger, although Traeger did note the likelihood of a kinetic shift in this case and excluded the propene onset from the data set used to derive the allyl ion heat of formation.

Interestingly, the rate of the H_2-loss relative to the H-loss increases with increasing internal excitation. Typically a simple bond cleavage will have a much looser transition state than a dissociation requiring a rearrangement, and will increasingly dominate the product branching at higher energies. However, the rate of a unimolecular dissociation increases with the number of modes that are converted from reactant vibrations into product rotations. In the case of an atom loss, only two vibrations (bends) are converted into product rotations. This number increases to four when one of the fragments is a linear molecule, and five when both fragments are nonlinear.

II. 3-Chloropropene. The breakdown diagram of 3-chloropropene taken at 235 K is shown in Figure 4, and associated TOF spectra are shown in Figure 5. It is evident from Figures 4 and 5 that the sole dissociation pathway below 11.4 eV is Cl-loss, and that the dissociation occurs slowly on the time scale of the experiment, necessitating rate information in order to determine E_0. The dissociation rate is embedded in the data in two ways. Similar to the propene data above, daughter ions produced in the initial acceleration region appear as an asymmetric peak originating at a TOF characteristic of the daughter mass. Also, $C_3H_5^+$ daughter ions produced from metastable parent ions in the first drift region appear as symmetric peaks at flight times longer than the parent ion. In this case, two partially resolved peaks appear corresponding to parent ions that contained the ^{35}Cl and ^{37}Cl isotopes. The abundance of these two peaks indicates the fraction of ions dissociating between 5.9 and 16.3 μs, while the abundance of the asymmetric peak indicates the fraction of ions dissociating within 5.9 μs of ionization. The relative areas of these peaks essentially determine two points on the unimolecular decay curve, and the data can be summarized by producing two breakdown curves: one reflecting dissociations occurring up until 5.9 μs, and the other all dissociations occurring up until 16.3 μs. The data is modeled using SSACM rate theory as described above.

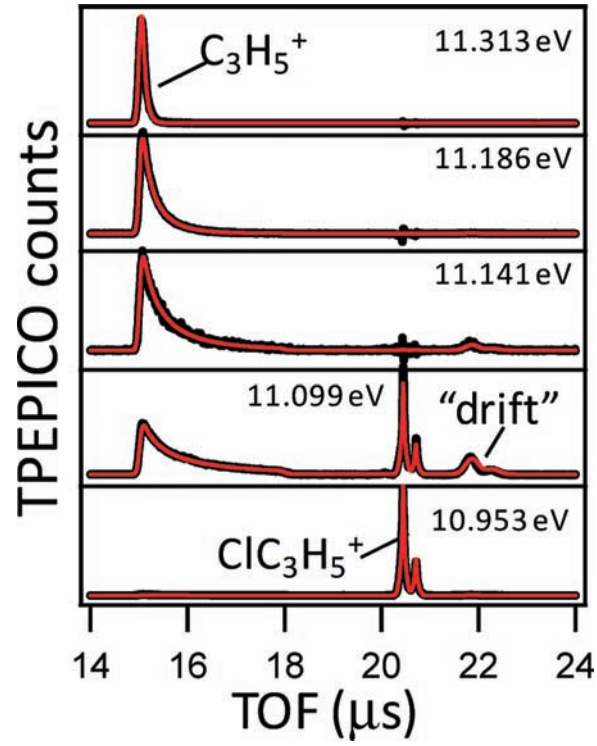

Figure 5. Experimental TOF spectra (black) and best fit simulations (red) of 3-ClC_3H_5 at the indicated photon energies.

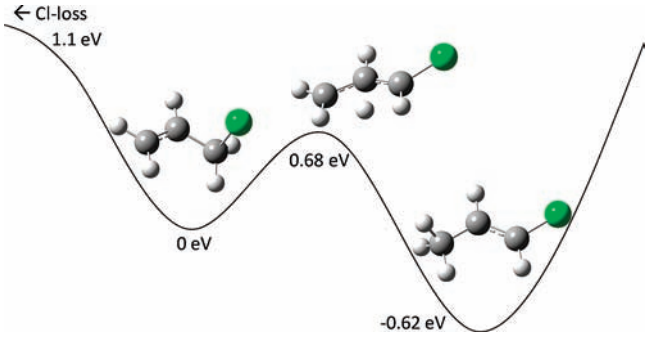

Figure 6. Stationary point structures and energetics of 3-$ClC_3H_5^+$ ↔ *trans*-1-$ClC_3H_5^+$ isomerization as calculated with the G3B3 model chemistry. Line serves only to guide the eye.

No acceptable fit to the data can be found by assuming that the dissociation occurs directly from the 3-chloropropene ion. However, excellent fits are found by assuming that 3-chloropropene ions rapidly isomerize to a lower energy isomer, such as the 2-chloropropene ion or *trans*- or *cis*- 1-chloropropene ions, all of which lie several hundred meV lower in energy. Isomerization to 2-chloropropene ion can be ruled out for several reasons: We observe H-loss and HCl-loss channels from 2-chloropropene ions (see below), but not from 3-chloropropene ions; the best-fit modeled rate curves for the two isomers are not identical; and we are unable to locate a transition state between the isomers using density functional calculations. On the other hand, transition states between the 3-chloropropene ion and both *cis*- and *trans*-1-chloropropene ions are found using the STQN method at the B3LYP/6-311++G(d,p) level, with both transition states involving a single hydrogen-transfer (Figure 6). The transition state to *trans*-1-chloropropene ion lies 400 meV below the experimental threshold to dissociation, while the transition state to *cis*-1-chloropropene ion lies 10 meV above the threshold, as calculated using the G3B3 model chemistry. Accordingly, we assume rapid isomerization to the *trans*-1-chloropropene ion in the analysis, the results of which are summarized in Table 2. Unfortunately, no data were collected on the *cis*- or *trans*-1-ClC_3H_5 systems in order to confirm or refute this mechanism. However, regardless of whether isomerization is assumed to *trans*- or *cis*-1-$ClC_3H_5^+$ or 2-$ClC_3H_5^+$, the best-fit E_0 varies by less than 10 meV (1 kJ mol^{-1}).

Modeling the isomerization requires the energy difference between the two structures. The heat of formation of *trans*-1-chloropropene ion has not been reported experimentally; instead we rely on a calculated energy difference using the G3B3 model chemistry (620 meV). Both the forward and reverse Rice−RRKM rate constants of the isomerization (assuming the calculated energies and transition state harmonic frequencies, and ignoring any tunneling contribution) are on the order of 10^8 s^{-1} at the dissociation threshold, orders of magnitude higher than the measured dissociation rate. Therefore, instead of explicitly modeling the isomerization rates, the populations of the isomers are assumed to be in equilibrium, and the density of states of the system is assumed to be equal to the sum of the densities of states of the two isomers.[36] The kinetics are effectively modeled by treating the system as dissociating directly from the much lower energy *trans*-1-chloropropene ion structure to the allyl ion because it provides the dominant contribution to the density of states.

III. 2-Chloropropene. Unlike the 3-chloropropene ion dissociation, we observe competing minor channels to Cl-loss from the 2-chloropropene ion. As shown in the TOF spectra in Figure 7, H-loss is observed at lower energies, and HCl-loss at higher

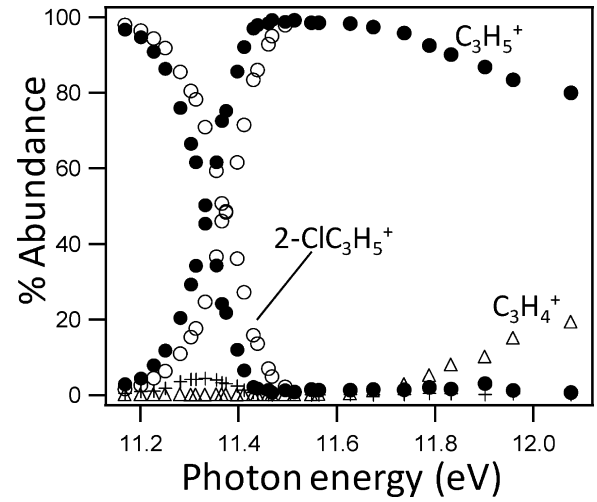

Figure 7. Experimental breakdown diagram of 2-$ClC_3H_5^+$ at 230 K. Parent and primary daughter ($C_3H_5^+$) ion abundances are shown for ion dissociations occurring within 5.9 μs of ionization (open circles) and those occurring within 16.3 μs (filled circles). Minor product channels ($C_3H_4^+$, open triangles; $ClC_3H_4^+$, crosses, unlabeled) are not fully resolved from larger peaks in the TOF spectra and shown abundances are approximate.

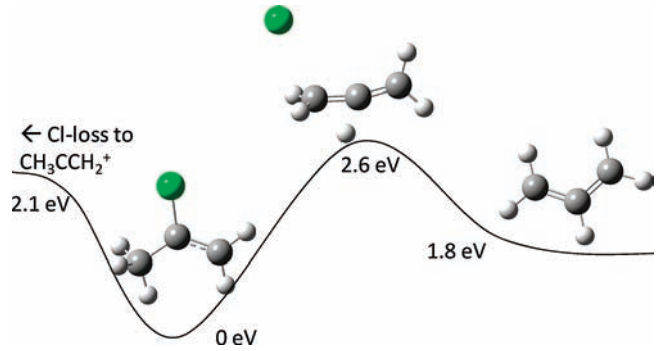

Figure 8. Structures and energetics of the proposed mechanism for the dissociation of 2-$ClC_3H_5^+$ to allyl ion. Relative energies are those calculated using the G3B3 model chemistry. Line serves only to guide the eye.

energies. The H-loss daughter peak is not entirely resolved from the parent ion peak, and the metastable HCl-loss peak is not entirely resolved from the Cl-loss peak, greatly complicating the analysis. By ignoring the minor channels in the modeling, we can approximate the E_0 for the $C_3H_5^+$ loss channel to be 11.35 eV. This is far too low an onset to be producing the 2-propenyl ion, rather the $C_3H_5^+$ structure produced from the 2-chloropropene ion must also be the allyl ion, probably via a single concerted step.

Calculations by the STQN method at the B3LYP/6-311++G(d,p) level suggest a possible mechanism in which a hydrogen atom from the 3-carbon attacks the 2-carbon from the reverse side, displacing the Cl and inverting the carbon backbone in an intramolecular S_N2 type mechanism (Figure 8). Although calculations using the G3B3 model chemistry suggest this transition state is higher in energy than the competing threshold to simple Cl-loss, the mechanism is still plausible due to possible tunneling through the reverse barrier. Because this reaction proceeds via a barrier, we cannot obtain any thermochemical information, and thus have chosen not to model the TOF distributions or the breakdown diagram.

TABLE 1: Derived and Ancillary Heats of Formation (kJ mol^{-1})

species	$\Delta H°_{f,0K}$	$H_{298K} - H_{0K}$[a]	$\Delta H°_{f,298K}$[b]	lit. $\Delta H°_{f,298K}$
C_3H_6	35.3	13.2		20.0 ± 0.7[c]
CH_2CHCH_2	182.7	12.5	170.9 ± 2.5	171 ± 4,[d] 173.2 ± 2.1[e]
$CH_2CHCH_2^+$	967.2	12.5	955.5 ± 2.5	949.6 ± 1.4[f]
$CH_3CCH_2^+$	997[g]	14.6	988	970 ± 10[h], 992[i]
3-ClC_3H_5	14.9	15.1	1.1 ± 2.7	-0.6[j]
2-ClC_3H_5	−7	15.0		-21 ± 9.4[c]
CH_3CCH	192.8	12.2		184.9 ± 0.7[c]
CH_2CCH_2	198.5	12.0		190.5 ± 1.1[c]

[a] The "ion convention" is followed (i.e., the heat capacity of a free electron is treated as 0 kJ mol^{-1} at all temperatures). [b] This work. [c] Pedley.[22] [d] Tsang,[4] for other values see text. [e] Ellison,[1] for other values see text. [f] Traeger,[5] for other values see text. [g] Calculated relative to allyl ion using G3, CBS-APNO, and W1 model chemistries. [h] Holmes et al.[19] [i] Bowers et al.[45] [j] Stull et al.[24]

Thermochemistry

The E_0 of H-loss from propene yields the 0 K heat of formation of the allyl ion ($\Delta H°_{f,0K} = 967.2 \pm 2.5$ kJ mol^{-1}), which can be converted to the 298 K ($\Delta H°_{f,298K} = 955.5$ kJ mol^{-1}) value by the standard thermochemical cycle (Table 1). Comparison to determinations of the 0 K heat of formation of the allyl radical suggests an IE of the radical of 8.11 ± 0.03 eV, in good agreement with the known value of 8.13146 ± 0.00025 eV. The current ion heat of formation forms a self-consistent data set with the more recently determined radical heat of formation and the known ionization energy. The discrepancy of 0.02 eV (2 kJ/mol) is a result of the experimental difficulties in establishing the allyl radical and ion heats of formation to higher precision. Because the allyl ion is closed shell, it may be possible to improve the precision by calculation of its heat of formation using high level calculations such as are afforded by either W4[43] or HEAT[44] methods.

As stated above, the photoionization of 2-chloropropene results in a concerted mechanism to eliminate Cl and rearrange to form the allyl ion. Because the dissociation must proceed over a barrier, no thermochemistry can be derived from a measured E_0. Although we are unable to report an experimental value for the $CH_3CCH_2^+$, calculations using the G3, CBS-APNO, and W1 model chemistries suggest a heat of formation 31, 29, and 29 kJ mol^{-1} higher than that of allyl ion, respectively. This 2-propenyl ion heat of formation ($\Delta H°_{f,0K} = 997$; $\Delta H°_{f,298K} = 988$ kJ mol^{-1}) is in excellent agreement with one previously reported experimental value ($\Delta H°_{f,298K} = 992$ kJ mol^{-1})[45] determined by equilibrium measurements, but significantly more positive than another previously reported value ($\Delta H°_{f,298K} = 970 \pm 10$ kJ mol^{-1}).[19] There are potential concerns with the latter experimental value: it is derived from collisonally induced dissociation measurements of 2-bromo- and 2-iodopropene, neither of which have well-established heats of formation, and, like the 2-chloropropene dissociation reported here, the structure of the $C_3H_5^+$ product may not be the 2-propenyl ion.

The allyl ion and 2-propenyl ion heats of formation define the proton affinities (PA) of C_3H_4 species. Assuming simple addition without rearrangement, proton addition to propyne yields the 2-propenyl ion, and proton addition to propadiene (allene) yields the allyl ion. Adopting the allyl ion heat of formation reported here and the 2-propenyl ion heat of formation reported by Bowers et al.,[45] the 298 K PA's are 723 and 765 kJ mol^{-1} respectively, in contrast to 748 and 775.3 kJ mol^{-1} reported in the compilation by Hunter and Lias.[46]

Photodissociation of 3-chloropropene results in production of the allyl ion and a chlorine atom at the thermochemical threshold. Because the heat of formation of the allyl ion is now well established, the measured E_0 can be used to derive the heat of formation of 3-chloropropene ($\Delta H°_{f,0K} = 14.9$, $\Delta H°_{f,298K} = 1.1 \pm 2.7$ kJ mol^{-1}). This is in somewhat poor agreement with the only value reported in the NIST Webbook ($\Delta H°_{f,298K} = -5.6$ kJ mol^{-1}), however this value was determined by Traeger[5] in the aforementioned PIMS study, and is superseded by the results here. The current number is in very good agreement with a value ($\Delta H°_{f,298K} = -0.6$ kJ mol^{-1}) reported in a compilation by Stull, Westrum, and Sinke,[24] taken as the average of an older enthalpy of combustion measurement[25] and a value derived from the difference in allyl ion appearance energies from 3-chloropropene and 3-iodopropene.[26]

The heats of formation of 2-chloropropene ($\Delta H°_{f,298K} = -21 \pm 9.4$ kJ mol^{-1})[22] and *cis*-($\Delta H°_{f,298K} = -15$ kJ mol^{-1})[47] and *trans*-1-chloropropene ($\Delta H°_{f,298K} = -12$ kJ mol^{-1})[47] have been determined by equilibria studies (i.e., not anchoring to the allyl ion). Both 1-chloropropene values were determined relative to the 3-chloropropene heat of formation using the value reported by Stull, Westrum, and Sinke,[24] and in light of the current results should be revised upward by 1.7 kJ mol^{-1}. Calculations using the G3B3 and CBS-APNO model chemistries are in reasonable agreement with these experimental results, suggesting that the 298 K heats of formation of 2-chloropropene and *cis*- and *trans*-1-chloropropene are 20, 11, and 8 kJ mol^{-1} more negative than that of 3-chloropropene, respectively.

Summary

A new value for the 0 K H loss onset from the propene ion has been obtained by taking into account the slow dissociation rate at the thermochemical threshold. The derived heat of formation of the resulting allyl ion, $\Delta H°_{f,298K} = 955.5 \pm 2.5$, is now in line with the latest allyl radical heat of formation and the very well established adiabatic ionization energy of the allyl radical. By using the allyl ion as a thermochemical anchor, we have determined the 3-chloropropene heat of formation from the measured E_0 for the Cl loss reaction. The slow rate of dissociation of this ion was also taken into account. Finally, the allyl ion heat of formation leads to a new allene proton affinity of 765 ± 2.6 kJ mol^{-1}.

Acknowledgment. We thank Michael Mautner for bringing potential issues in the $C_3H_5^+$ thermochemistry to our attention. We thank the U.S. Department of Energy, Office of Basic Energy Sciences, for financial support.

References and Notes

(1) Ellison, G. B.; Davico, G. E.; Bierbaum, V. M.; DePuy, C. H. *Int. J. Mass Spectrom. Ion. Processes* **1996**, *156*, 109–131.
(2) Rossi, M.; King, K. D.; Golden, D. M. *J. Am. Chem. Soc.* **1979**, *101* (5), 1223–1230.
(3) Rossi, M.; Golden, D. M. *J. Am. Chem. Soc.* **1979**, *101* (5), 1230–1235.
(4) Tsang, W.; Walker, J. A. *J. Phys. Chem.* **1992**, *96* (21), 8378–8384.
(5) Traeger, J. C. *Int. J. Mass Spectrom. Ion. Processes* **1984**, *58*, 259–271.
(6) Lossing, F. P. *Can. J. Chem.* **1972**, *50* (24), 3973–3981.
(7) Buttrill, S. E.; Williamson, A. D.; Lebreton, P. *J. Chem. Phys.* **1975**, *62* (4), 1586–1587.
(8) Meisels, G. G.; Park, J. Y.; Giessner, B. G. *J. Am. Chem. Soc.* **1970**, *92* (2), 254.
(9) Fischer, I.; Schussler, T.; Deyerl, H. J.; Elhanine, M.; Alcaraz, C. *Int. J. Mass Spectrom.* **2007**, *261* (2−3), 227–233.
(10) Xing, X.; Reed, B.; Lau, K. C.; Ng, C. Y.; Zhang, X.; Ellison, G. B. *J. Chem. Phys.* **2007**, *126* (17), 171101/1-171101/4.

(11) Gilbert, T.; Fischer, I.; Chen, P. *J. Chem. Phys.* **2000**, *113* (2), 561–566.
(12) Houle, F. A.; Beauchamp, J. L. *J. Am. Chem. Soc.* **1978**, *100*, 3290–3294.
(13) Wu, J. C.; Li, R. H.; Chang, J. L.; Chen, Y. T. *J. Chem. Phys.* **2000**, *113* (17), 7286–7291.
(14) Liang, C. W.; Chen, C. C.; Wei, C. Y.; Chen, Y. T. *J. Chem. Phys.* **2002**, *116* (10), 4162–4169.
(15) Lau, K. C.; Ng, C. Y. *J. Chem. Phys.* **2006**, *124* (4), 044323/1-044323/9.
(16) Lau, K. C.; Ng, C. Y. *Acc. Chem. Res.* **2006**, *39* (11), 823−829.
(17) Gasser, M.; Schulenburg, A. M.; Dietiker, P. M.; Bach, A.; Merkt, F.; Chen, P. *J. Chem. Phys.* **2009**, *131*, 014304.
(18) Benson, S. W. *Thermochemical Kinetics*, 2nd ed.; John Wiley & Sons: New York, 1976.
(19) Holmes, J. L.; Aubry, C.; Mayer, P. M. *Assigning Structures to Ions in Mass Spectrometry*; CRC Press: Boca Raton, FL, 2007.
(20) Steiner, B. W.; Giese, C. F.; Inghram, M. G. *J. Chem. Phys.* **1961**, *34*, 189–220.
(21) Chupka, W. A. *J. Chem. Phys.* **1959**, *30*, 191–211.
(22) Pedley, J. B. *Thermochemical Data and Structures of Organic Compounds*; Thermodynamics Research Center: College Station, 1994.
(23) Bowers, M. T.; Shuying, L.; Kemper, P.; Stradling, R.; Webb, H.; Aue, D. H.; Gilbert, J. R.; Jennings, K. R. *J. Am. Chem. Soc.* **1980**, *102*, 4830–4832.
(24) Stull, D. R.; Westrum, E. F., Jr.; Sinke, G. C. *The Chemical Thermodynamics of Organic Compounds*; John Wiley and Sons, Inc.: New York, 1969.
(25) Karasch, M. S. *J. Res. Nat. Bur. Stand. (U.S.)* **1929**, *2*, 359.
(26) Lossing, F. P.; Ingold, K. U.; Henderson, I. H. S. *J. Chem. Phys.* **1954**, *22*, 1489.
(27) Shevtsova, L. A.; Rozhnov, A. M.; Andreevskii, D. N. *Russ. J. Phys. Chem. (Engl. Transl.)* **1970**, *44*, 852–855.
(28) Baer, T.; Li, Y. *Int. J. Mass Spectrom.* **2002**, *219*, 381–389.
(29) Sztáray, B.; Baer, T. *Rev. Sci. Instrum.* **2003**, *74*, 3763–3768.
(30) Kercher, J. P.; Stevens, W.; Gengeliczki, Z.; Baer, T. *Int. J. Mass Spectrom.* **2007**, *267*, 159–166.
(31) Gaussian 03, Revision C.02, Gaussian, Inc.: Wallingford, CT, 2004.
(32) Merrick, J. P.; Moran, D.; Radom, L. *J. Phys. Chem. A* **2007**, *111*, 11683–11700.
(33) Baboul, A. G.; Curtiss, L. A.; Redfern, P. C.; Raghavachari, K. *J. Chem. Phys.* **1999**, *110* (16), 7650–7657.
(34) Ochterski, J. W.; Petersson, G. A.; Montgomery, J. A. *J. Chem. Phys.* **1996**, *104* (7), 2598–2619.
(35) *NIST Chemistry WebBook, NIST Standard Reference Database Number 69*; February 2000 ed.; National Institute of Standards and Technology: 2005.
(36) Baer, T.; Hase, W. L. *Unimolecular Reaction Dynamics: Theory and Experiments*; Oxford University Press: New York, 1996.
(37) Hase, W. L. *J. Chem. Phys.* **1976**, *64*, 2442–2449.
(38) Chesnavich, W. J.; Bass, L.; Su, T.; Bowers, M. T. *J. Chem. Phys.* **1981**, *74*, 2228–2246.
(39) Troe, J. *J. Chem. Phys.* **1987**, *87*, 2773–2780.
(40) Troe, J.; Ushakov, V. G.; Viggiano, A. A. *J. Phys. Chem. A* **2006**, *110*, 1491–1499.
(41) Stevens, W.; Sztáray, B.; Shuman, N.; Baer, T.; Troe, J. *J. Phys. Chem. A* **2009**, *113*, 573–582.
(42) Baer, T.; Sztáray, B.; Kercher, J. P.; Lago, A. F.; Bodi, A.; Scull, C.; Palathinkal, D. *Phys. Chem. Chem. Phys.* **2005**, *7*, 1507–1513.
(43) Karton, A.; Rabinovich, E.; Martin, J. M. L.; Ruscic, B. *J. Chem. Phys.* **2006**, *125*, 144108−1–144108/17.
(44) Harding, M. E.; Vazquez, J.; Ruscic, B.; Wilson, A. K.; Gauss, J.; Stanton, J. F. *J. Chem. Phys.* **2008**, *128*, 114111-1–114111-15.
(45) Aue, D. H.; Davdidson, W. R.; Bowers, M. T. *J. Am. Chem. Soc.* **1976**, *98* (21), 6700–6702.
(46) Hunter, E. P. L.; Lias, S. G. *J. Phys. Chem. Ref. Data* **1998**, *27*, 413–656.
(47) Alfassi, Z. B.; Golden, D. M.; Benson, S. W. *J. Chem. Thermodyn.* **1973**, *5*, 411–420.

JP906691A